

Published in final edited form as:

Free Radic Biol Med. 2011 May 1; 50(9): 1163–1170. doi:10.1016/j.freeradbiomed.2011.02.001.

Characterization of Free Radicals Formed from COX-Catalyzed DGLA Peroxidation

Ying Xiao^{a,b}, Yan Gu^b, Preeti Purwaha^b, Kunyi Ni^a, Benedict Law^b, Sanku Mallik^b, and Steven Y. Qian^{b,*}

^aDepartment of Analytical Chemistry, China Pharmaceutical University, Nanjing 210009, China

^bDepartment of Pharmaceutical Sciences, College of Pharmacy, Nursing, and Allied Sciences, North Dakota State University, Fargo, ND 58105, USA

Abstract

Like arachidonic acid (AA), dihomo- γ -linolenic acid (DGLA) is a 20-carbon ω -6 polyunsaturated fatty acid and a substrate of cyclooxygenase (COX). Through free radical reactions, COX metabolizes DGLA and AA to form well-known bioactive metabolites, namely, the 1- and 2-series of prostaglandins (PGs1 and PGs2), respectively. Unlike PGs2, which are viewed as pro-inflammatory, PGs1 possess anti-inflammatory and anticancer activities. However, the mechanisms linking the PGs to their bioactivities are still unclear, and radicals generated in COX-DGLA have not been detected. In order to better understand PGs biology and determine whether different reactions occur in COX-DGLA than in COX-AA, we have used LC/ESR/MS with a spin trap, α -[4-pyridyl-1-oxide]-N-*tert*-butyl nitron (POBN), to characterize the carbon-centered radicals formed from COX-DGLA in vitro, including cellular peroxidation. A total of five types of DGLA-derived radicals were characterized as POBN adducts: m/z 266, m/z 296 and m/z 550 (same as and/or similar to COX-AA), and m/z 324 and m/z 354 (exclusively from COX-DGLA). Our results suggested that C-15 oxygenation to form PGGs occurs in both COX-DGLA and COX-AA; however, C-8 oxygenation occurs exclusively in COX-DGLA. This new finding will be further investigated for its association with different bioactivities of PGs, with potential implications for inflammatory diseases.

Keywords

ESR spin-trapping; DGLA-derived radicals; COX-catalyzed peroxidation; cellular (HCA-7 Colony 29) peroxidation; on-line LC/ESR, LC/MS, and LC/MS²

INTRODUCTION

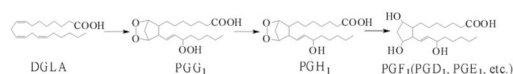
Dihomo- γ -linolenic acid (DGLA) is a 20-carbon ω -6 PFUA derived in vivo from linolenic acid (LA), an essential fatty acid. DGLA can then be converted to arachidonic acid (AA), another 20-carbon ω -6 polyunsaturated fatty acid (PUFA) [1,2]. Both DGLA and AA are substrates of the lipid peroxidizing enzyme COX. Through a series of free radical reactions,

*Corresponding Author: Steven Y. Qian, Ph.D., Department of Pharmaceutical Sciences, College of Pharmacy, Nursing, and Allied Sciences, North Dakota State University, Fargo, ND 58105, USA, Tel: (701) 231-8511, Fax: (701) 231-8333, steven.qian@ndsu.edu.

Publisher's Disclaimer: This is a PDF file of an unedited manuscript that has been accepted for publication. As a service to our customers we are providing this early version of the manuscript. The manuscript will undergo copyediting, typesetting, and review of the resulting proof before it is published in its final citable form. Please note that during the production process errors may be discovered which could affect the content, and all legal disclaimers that apply to the journal pertain.

COX metabolizes DGLA and AA to form different bioactive metabolites, namely, the 1- and the 2-series of prostaglandins (PGs1 and PGs2), respectively. Unlike PGs2, which are generally viewed as pro-inflammatory PGs [3–5], PGs1 actually possess anti-inflammatory and anticancer activities. For example, PGE1, one form of PGs1, could inhibit vascular smooth muscle cell proliferation, reduce vascular cell adhesion, and attenuate the development of atherosclerosis [6–10].

Although much research attention has been focused on the study of PGs bioactivity [3–12], the mechanism linking the structure of PGs to their bioactivity is still unclear, and the free radicals generated in COX-DGLA have never been detected due to the lack of appropriate methodologies. As in COX-AA peroxidation, several free radical reactions are involved in the formation of PGG1 from DGLA, e.g. formation of C-13 radical (the initial step), introduction of O₂ on C-11 to form C-9/C11 endoperoxide, C-8/C-12 cyclization (creation of a carbon bond between C-8 and C-12), and 15-C peroxidation (addition of the second O₂ to the DGLA molecule) [13–16]. PGG1 can then be readily transformed into PGH1, PGE1 and PGF1 α (Reaction 1) [15–16].



(Reaction 1)

However, it is still unclear whether different free radical reactions occur in COX-AA and COX-DGLA peroxidation, and whether these differences are associated with the bioactivity of PGs and fatty acids.

Recently, we have successfully used the combination of LC/ESR and LC/MS to identify the radicals formed from COX-AA peroxidation and have observed that free radicals were formed from a special β -scission during COX-AA peroxidation [17]. In the present study, in order to determine whether different free radical reactions occur in COX-catalyzed DGLA than in AA peroxidation, a combination of LC/ESR and LC/MS was again applied to characterize DGLA-derived radicals formed from COX-DGLA in vitro, including cellular (human colon cancer cell line HCA-7 Colony 29) peroxidation, in the presence of the spin trap α -[4-pyridyl]-1-oxide]-N-*tert*-butyl nitron (POBN).

In addition to forming similar free radicals via the same pathway reported in COX-AA [17], unique radical reactions were also observed in COX-DGLA. A total of five types of DGLA-derived radicals were characterized as POBN adducts, including three types that were the same or similar to those formed in COX-AA: m/z 266 (POBN/[•]C₅H₁₁), m/z 296 (POBN/[•]C₆H₁₃O), and m/z 550 (POBN/[•]C₂₀H₃₅O₅); and two types formed exclusively in COX-DGLA: m/z 354 (POBN/[•]C₈H₁₅O₃) and m/z 324 (POBN/[•]C₇H₁₃O₂). The results of our studies suggested that the C-15 oxygenation to form PGGs (Reaction 1) appears to occur in both COX-mediated DGLA and AA peroxidation, while C-8 oxygenation forming related peroxides occurs exclusively in COX-DGLA. We will further investigate the association of these new products with PGs bioactivity and assess their potential implications for inflammatory diseases.

MATERIALS AND METHODS

Reagents

Ethyl alcohol, glacial acetic acid (HOAc), hydroquinone, and porcine hematin were purchased from Sigma Chemical Co. (St. Louis, MO, USA). Acetonitrile (ACN; HPLC grade) and Tris-(hydroxymethyl) aminomethane were obtained from Mallinckrodt Baker

(Phillipsburg, NJ, USA). LC/MS grade water (H₂O) was purchased from EMD Chemicals (Gibbstown, NJ, USA). COX-2 enzyme (ovine) and DGLA were purchased from Cayman Chemical (Ann Arbor, MI, USA). Chelex 100 (200–400 mesh sodium form) was bought from Bio-Rad Laboratories (Hercules, CA, USA). High-purity POBN was purchased from Alexis Biochemicals (San Diego, CA, USA), and deuterated POBN (D₉-POBN) was obtained from CDN Isotopes (Pointe-Claire, QC, Canada). The human colon cancer cell line, HCA-7 Colony 29, was purchased from European Collection of Cell Cultures (ECACC, Porton Down, Salisbury, UK). HyClone[®] DMEM high glucose medium was obtained ThermoFisher Scientific (Logan, Utah). Fetal bovine serum (FBS) and trypsin-EDTA were purchased from GIBCO BRL (Grand Island, NY, USA).

Reaction conditions

The reactions of COX catalysis of DGLA were performed in 0.1 M (pH 8.0) “metal-free” Tris-Cl buffer solutions. Metal ions in the Tris-Cl buffer solution were chelated by treatment with Chelex 100 resin to provide a virtually metal-free buffer solution, which passed an ascorbic acid test. A reaction mixture containing 5 Kunit/mL COX enzyme, 100 mM POBN, and 50 μM hematin was pre-incubated for 5 minutes at 37°C and 600 rpm on a Thermo-Shaker (Boekel Scientific, Feasterville, PA). Five mM hydroquinone and 2 mM DGLA (in ethanol) were then added to start the reaction. This complete reaction mixture (~1% ethanol, v/v, from a DGLA stock solution) was then incubated at 37°C and 600 rpm on a Thermo-Shaker in the absence of light. After a 30 min incubation, the COX-catalyzed peroxidation was immediately stopped by mixing with same amount of ACN and was centrifuged and condensed for later LC/ESR and LC/MS analysis as described elsewhere.

Free radicals from cellular COX-mediated peroxidation were generated with HCA-7 Colony 29 cells grown in HyClone[®] DMEM high glucose medium supplemented with 10% FBS in an incubator containing a humidified atmosphere of 5% CO₂ at 37°C. At 70–80% confluence, the cells were trypsinized, harvested, and suspended in phosphate buffer saline (PBS) ~10⁷ cells/mL. POBN and DGLA at final concentrations of 50 mM and 0.1 mM–1.0 mM, respectively, were then added to the cell suspension to start the DGLA peroxidation and POBN spin-trapping reaction. After a 30-min incubation, the peroxidation of cell suspension was stopped with ACN (1:1 v/v), and then supernatant was collected, centrifuged and condensed for LC/ESR and LC/MS analysis.

On-line LC/ESR measurements

The on-line LC/ESR system consisted of an Agilent 1200 series HPLC system and a Bruker EMX ESR system. The outlet of the Agilent UV detector was connected to a highly sensitive Aquax ESR cell with red PEEK HPLC tubing (0.005 i.d.). The POBN radical adducts were monitored *via* UV absorption at 265 nm followed by ESR detection. There was a delay of about 9 s between the UV and the ESR detection in our on-line LC/ESR settings. LC separations were performed on a C18 column (Zorbax Eclipse-XDB, 4.6×75 mm, 3.5 μm) and a guard column (Zorbax Eclipse-XDB, 4.6×12.5 mm, 5 μm) equilibrated with 90% A (H₂O–0.1% HOAc) and 10% B (ACN–0.1% HOAc). Forty microliters of enzyme-free condensed sample was injected into the HPLC system by autosampler and eluted at a 0.8 ml/min flow rate with a combination of gradient and isocratic elution: (1) 0–6 min: 100% to 75% of A and 0% to 25% of B; (2) 6–18 min (isocratic): 75% of A and 25% of B; (3) 18–40 min: 75% to 30% of A and 25% to 70% of B; (4) 40–43 min: 30% to 5% of A and 70% to 95% of B; and (5) 43–50 min (isocratic): 5% of A and 95% of B. On-line ESR measurements were performed using a time scan mode with the magnetic field (~3498 G) fixed on the maximum of the first line of the six-line spectrum of the POBN adduct as described elsewhere [17,19–21]. Other ESR settings were modulation frequency, 100 kHz;

modulation amplitude, 3.0 G; microwave power, 20 mW; receiver gain, 4×10^5 ; and time constant, 2.6 s.

On-line LC/MS and LC/MS² measurements

The LC/MS system consisted of an Agilent 1200 series HPLC system and an Agilent LC/MSD SL iron trap mass system. The outlet of the UV detector in LC was connected to the MS system with red PEEK HPLC tubing as well. Chromatographic conditions were identical to those used for on-line LC/ESR. However, the LC flow rate (0.8 ml/min) into the MS inlet was adjusted to 30–40 μ l/min via a splitter. There was a delay of \sim 35 s between the UV and the MS detection in our on-line LC/MS settings. Electrospray ionization (ESI) in positive mode was used for all LC/MS and LC/MS² measurements unless otherwise specified. Total ion current (TIC) chromatograms in full mass scan mode (m/z 50 to m/z 600) were performed to profile all products formed in the reaction of COX-catalyzed DGLA in vitro in the presence of POBN. Other MS settings were capillary voltage, -4500 V; nebulizer press, 20 psi; dry gas flow rate, 8 L/min; dry temperature, 60°C; compound stability, 20%; and number of scans, 50. Extracted ion current (EIC) chromatograms of ions of interest were projected from TIC to acquire MS chromatograms that could match well with ESR chromatograms, in which all POBN radical adducts were monitored as structure nonspecific ESR-active peaks. EIC was also performed to determine the number of isomers of given ions. Normally an isolation width of ± 0.5 Da was selected for EICs. The multiple reaction monitoring mode of LC/MS² was conducted to confirm structural assignments of POBN adducts. A width of ± 2.0 Da was typically selected to isolate parent ions of interest.

RESULTS

When off-line ESR (magnetic field scan) was used to measure free radical adducts in the COX-DGLA complete reaction mixture, we obtained a mixed spectrum (data not shown) composed of a six-line ESR signal of POBN radical adducts ($a^N \approx 15.33$ G and $a^H \approx 2.39$ G) and an overlapping five-line ESR signal in the center from benzosemiquinone radicals generated from hydroquinone oxidation as described elsewhere [17]. However, the off-line ESR measurement can provide only an overall signal intensity of radical adducts, not specific information in terms of types, numbers, and structures, since many of the POBN spin adducts tend to have the same or similar hyperfine couplings of a^N and a^H [24].

When we used the combined techniques of on-line LC/ESR and LC/MS to further examine more specific radical information from the COX-DGLA complete reaction mixture, we observed a total of thirteen ESR-active peaks corresponding to different POBN radical adducts (include isomers) (Figure 1B). Among these ESR-active peaks, some (peaks 2, 3, 4, 7, 12, and 13) were matched with their corresponding UV peaks (Figure 1A, asterisked peaks), while for others (peaks 1, 5, 6, 8, 9, 11, and 12) the corresponding UV could not be observed.

The extracted ion chromatogram (EIC) of four protonated molecular ions of m/z 354, m/z 324, m/z 296 and m/z 266 could be projected from the full MS scan (m/z 50- m/z 600, Figure 1C) of the COX-DGLA complete reaction mixture. It matches the profile of major ESR-active peaks (peaks 2, 3, 4, 7, 12, and 13) very well, indicating that there are four main types of DGLA-derived radicals formed in the COX-DGLA system and trapped by POBN.

Due to sharing the same structural moiety (C-8 to C-20) as AA, the m/z 266 and m/z 296 radical adducts were also observed in COX-DGLA as ESR-active peak 13 (EIC of m/z 266, $t_R \approx 25.7$ min, Figure 1C and Figure 2A) and the two ESR-active peaks 7 and 12 (EIC of m/z 296, $t_R \approx 16.3$ and 23.6 min, Figure 1C and Figure 2B), respectively. They most likely correspond to the POBN adducts of pentyl radical ($\cdot C_5H_{11}$) and two isomers of hexanol

radicals ($\text{C}_6\text{H}_{13}\text{O}$) generated in the COX-DGLA reaction as proposed in Scheme 1. The structure assignments were confirmed by their LC/MS² analysis (Figures 2C and 2D), as their fragment patterns all agreed with the patterns published previously [17] as well as with the patterns observed in D₉-POBN spin-trapping experiments (data not shown).

Unlike the m/z 266 and m/z 296 molecules common in DGLA and AA peroxidation, molecules of m/z 354 and m/z 324 (ESR-active peaks 2–3 and 4) most likely correspond to radicals formed either from different structural moieties (C-1 to C-8) and/or via free radical reactions that differ in COX-DGLA vs. COX-AA. They appear to be the adducts of $\text{C}_8\text{H}_{15}\text{O}_3$ and $\text{C}_7\text{H}_{13}\text{O}_2$, respectively, and the EIC peaks were projected at $t_R \approx 9.6$, 10.9, and 11.8 min (Figure 1C and Figures 3–4).

ESR-active peaks 2–3 and the corresponding EIC peaks ($t_R \approx 9.6$ and 10.9 min, m/z 354, Figure 1C and Figure 3A) appear to be two isomers of a POBN adduct of a $\text{C}_8\text{H}_{15}\text{O}_3$ radical with a carboxyl end which formed from β '-scission of a DGLA-derived alkoxy radical as proposed in Scheme 2. The presence of the isomers of such an adduct was confirmed by the presence of two m/z 363 peaks in the EIC of a D₉-POBN experiment ($t_R \approx 9.5$ and 10.8 min, Figure 3B). The fragmentation pattern shown in the LC/MS² of m/z 354 and m/z 363 (Figures 3C and 3D) further confirmed the structure assignment as a POBN adduct of $\text{C}_8\text{H}_{15}\text{O}_3$. However, there was not enough evidence from the fragmentation ions in LC/MS² of peaks 2–3 (two isomers of m/z 354) to distinguish their differences.

The ESR-active peak 4 and its EIC peaks ($t_R \approx 11.8$ min, m/z 324, Figure 1C and Figure 4A) appeared to be the POBN adduct of $\text{C}_7\text{H}_{13}\text{O}_2$ with the carboxyl end which formed from β -scission of the DGLA-derived alkoxy radical as proposed in Scheme 2 as well. The EIC of the m/z 333 peak ($t_R \approx 11.6$ min, Figures 4B) was then observed in the D₉-POBN experiment, and the structure assignment of this radical adduct was further confirmed by observing a similar fragmentation pattern in the LC/MS² analysis of m/z 324 and m/z 333 (Figures 4C–4D).

The first ESR-active peak ($t_R \approx 7.5$ min, Figure 1B), a DGLA-unrelated radical adduct, corresponded to the formation of the POBN-trapped hydroxyethyl radical ($\text{C}_2\text{H}_4\text{OH}$) from oxidation of ethanol, since 1% ethanol was always used to prepare the fatty acid stock solution for our reaction system. The LC/MS² of its m/z 240 (data not shown) matched the LC/MS² fragmentation pattern of POBN/ $\text{C}_2\text{H}_4\text{OH}$ published previously.

Despite a considerable effort, we were unable to match the intensities of the EIC projections of the rest of the ESR-active peaks (peaks 5, 6, 8, 9, 11, and 12) to their relative ESR intensities (Figure 1C); the MS responses (abundances) of these radical adducts appear to be much lower than the MS responses of m/z 296, m/z 266, m/z 324, and m/z 354. However, when the EIC of m/z 550 was projected alone, it closely matched a profile of the other six ESR-active peaks ($t_R \approx 12.6$, 14.8, 17.0, 18.8, 21.5 and 22.9 min, Figure 5A). The molecule of m/z 550 most likely corresponds to a PGF1-type radical (POBN/ $\text{C}_{20}\text{H}_{35}\text{O}_5$) as proposed in Scheme 1. The similar EIC of m/z 559, obtained from a D₉-POBN spin trapping experiment ($t_R \approx 12.4$, 14.6, 16.7, 18.3, 21.0 and 22.6 min, Figure 5B), and LC/MS² analysis of m/z 550 and m/z 559 (Figures 5C–5D) further confirmed this assignment. However, again, there was not enough evidence from the LC/MS² analysis of those fractions to distinguish between the isomers.

The human colon cancer cell line HCA-7 Colony 29 is a new addition to the colorectal collection that could be particularly effectively used for PGs research due to its higher expression of COX-2. When HCA-7 Colony 29 cells were incubated with both DGLA and POBN, a typical six-line signal of POBN adduct was observed ($a^N \approx 15.72$ G and $a^H \approx 2.55$ G), but low detection sensitivity of the LC/ESR resulted in poor on-line ESR

chromatography (data not shown). However, four main radical adducts were clearly projected from the full MS analysis of cellular peroxidation in the presence of DGLA and POBN as shown in their individual EICs (Figure 6). These four radical adducts are m/z 266 (peak at 25.7 min, Figure 6A), two isomers of m/z 296 (peaks at 16.3 and 23.6 min, Figure 6B), m/z 324 (peak at $t_R \approx 11.8$ min, Figure 6C), and two isomers of m/z 354 (peaks at $t_R \approx 9.6$ and 10.9 min, Figure 6D). In addition to observing the same fragmentation pattern in their individual LC/MS² as those of the corresponding adducts in Figures 2–5, these radicals were also trapped and observed in the cellular experiment in the presence of D₉-POBN (data not shown). Thus, COX-2 mediated peroxidation of HCA-7 Colony 29 cells metabolizes DGLA as proposed in Schemes 1–2.

DISCUSSION

Both DGLA and AA are 20-carbon carbon ω -6 polyunsaturated fatty acids (PUFAs) and substrates of COX. However, their metabolites, e.g. PGs1 and PGs2, may have opposite bioactivity. We have recently identified novel free radicals formed from COX-AA peroxidation using a combination of LC/ESR and LC/MS [17]. Understanding these radicals and related radical reactions may allow us to advance our knowledge of COX biology. The purpose of this research is to study similar and different free radical reactions undergoing COX-mediated DGLA vs. COX-AA peroxidation, thus laying the foundation for our future studies on the mechanisms linking the structures of PGs and fatty acids to their bioactivity.

We have now used the combination technique of LC/ESR and LC/MS to characterize the spin adducts of carbon-centered radicals formed from COX-catalyzed DGLA peroxidation in the presence of POBN. A total of five types of DGLA-derived radicals were identified, including four fragmented free radicals derived from β -scission of different alkoxy radicals and many isomers of PGF1-type carbon-centered radicals as proposed in Schemes 1–2.

Because both AA and DGLA share the same structural C-8 to C-20 moiety, COX can catalyze their free radical reactions in the same order: C-13 radical formation, C-9/C-11 endoperoxidation, C-8/C-12 cyclization, and C-15 oxygenation to form PGGs [13,15,27–28]. Similar to the reactions of COX-AA, normal β -scission of a PGH1-type alkoxy radical leads to the formation of a carbon-centered radical, $\cdot\text{C}_5\text{H}_{11}$ (m/z 266 for the adduct), while the special β' -scission of a PGH1-type alkoxy radical results in the formation of $\cdot\text{C}_6\text{H}_{13}\text{O}$ (m/z 296 for the adduct) from DGLA as shown in Scheme 1. However, unlike COX-AA peroxidation, in which a special β' -scission of a PGF2-type alkoxy radical also leads to formation of a carbon-double bond radical as the second radical besides $\cdot\text{C}_6\text{H}_{13}\text{O}$ (m/z 296 for the adduct) [17], this second radical was not observed in COX-DGLA peroxidation. In COX-DGLA peroxidation the β' -scission appears to preferably occur at PGH1 stage, which results in measurement of only the $\cdot\text{C}_6\text{H}_{13}\text{O}$ radical from this pathway. The second carbon-centered radical formed is readily rearranged to the oxygen-centered radical with a PGH1-endoperoxide bridge as proposed in Scheme 1. In general, POBN is unable to trap oxygen-centered radicals. We observed much less of the PGF1-type radical $\cdot\text{C}_{20}\text{H}_{35}\text{O}_5$ (m/z 550 for the adduct) from COX-DGLA in this study than the corresponding PGF2-type radicals (m/z 548 for POBN/ $\cdot\text{C}_{20}\text{H}_{33}\text{O}_5$) in COX-AA [17]; this observation appears to be consistent with our proposed mechanism (Scheme 1) in which the β' -scission most likely occurs at PGH1 (Scheme 1), rather than at PGF1. The difference between COX-AA and DGLA peroxidation regarding the generation of the second radical ($\cdot\text{C}=\text{C}$) from the special β' -scission will be further investigated for the links with their individual bioactivities.

The C-1 to C-7 segment of DGLA, a different structural moiety than that in AA, formed fragmented free radicals (from β -scission) at the carboxyl end exclusively in COX-DGLA peroxidation. Two such types of radicals, $\cdot\text{C}_8\text{H}_{15}\text{O}_3$ (m/z 354 for the adduct) and $\cdot\text{C}_7\text{H}_{13}\text{O}_2$

(m/z 324 for the adduct), are generated as proposed in Scheme 2. Thus, after the formation of the C-9/C-11 endoperoxide bridge, both 15-oxygenation (following C-8/C-12 cyclization) and C-8 oxygenation (before C-8/C-12 cyclization) can further carry over to the peroxidation of DGLA. The larger distances between C-7 and C-10 in DGLA compared to AA in the COX/substrate structure may explain why C-8 oxygenation occurs exclusively in COX-DGLA [29–30]. The formation of the carboxyl end radicals from C-8 oxygenation of DGLA was also confirmed by observing two isomers of m/z 368 (m/z 354 + with 14 Da, as POBN/ $^*C_9H_{17}O_3$, $t_R \approx 14.9$ and 21.6 min) and one m/z 338 (m/z 324 + 14 Da, as POBN/ $^*C_8H_{15}O_2$, $t_R \approx 23.6$ min) molecule by LC/MS analysis when DGLA-methyl ester was used to replace DGLA as a substrate in COX peroxidation (data not shown, Scheme 2). Although autoxidation of DGLA could be another possible pathway of C-8 oxygenation, our observation of C-8 oxygenation-related DGLA-derived radicals, e.g. $^*C_8H_{15}O_3$ and $^*C_7H_{13}O_2$, only in the COX-DGLA system, and not in the control experiments when COX was absent (data not shown), suggests that C-8 oxygenation should also be considered a COX-mediated pathway.

The β' -scission of alkoxy radicals derived from 8-OOH endoperoxide would be expected to form a complementary pair of carbon-centered radicals. However, only the $^*C_8H_{15}O_3$ radical was observed. We believe that the second carbon-centered radical with the C-9/C-11 endoperoxide bridge rearranges structurally to convert to an oxygen-centered radical as proposed in Scheme 2. Note that both proposed oxygen-centered radicals in Schemes 1–2 could further undergo C-9 and C-11 elimination to decompose to the other products, including malonaldehyde, a well known bioactive product. We are investigating the association of PGs bioactivity with the proposed free radicals and other products generated from COX-catalyzed AA and DGLA peroxidation in our laboratory. A better understanding of their respective bioactivities will advance our knowledge of COX and PGs biology and may have implications for inflammatory diseases.

Acknowledgments

This work was supported by NIH Grant K22ES-012978, 1R15CA140833, and P20 RR015566. We also appreciate China Pharmaceutical University's support of part of Ms. Xiao's salary.

LIST OF ABBREVIATIONS

AA	arachidonic acid
COX	Cyclooxygenase
DGLA	Dihomo- γ -linolenic acid
EIC	Extracted Ion Current
ESR	Electron Spin Resonance
HPLC (LC)	High Performance Liquid Chromatography
MS	Mass Spectrometry
PGs	Prostaglandins
POBN	α -[4-pyridyl-1-oxide]- <i>N</i> - <i>tert</i> -butyl nitron
t_R	Retention time
TIC	Total Ion Current

REFERENCES

1. Das UN. Essential fatty acids: biochemistry, physiology and pathology. *Biotechnol. J.* 2006; 1:420–439. [PubMed: 16892270]
2. Fan YY, Chapkin RS. Importance of dietary γ -linolenic acid in human health and nutrition. *J. Nutr.* 1998; 128:1411–1414. [PubMed: 9732298]
3. Sales KD, Katz AA, Davis M, Hinz S, Soeters RP, Hofmeyr MD, Millar RP, Jabbour HN. Cyclooxygenase-2 expression and prostaglandin E₂ synthesis are up-regulated in carcinomas of the cervix: a possible autocrine/paracrine regulation of neoplastic cell function via EP2/EP4 receptor. *J. Clin. Endocrinol. Metab.* 2001; 86:2243–2249. [PubMed: 11344234]
4. Lee LM, Pan CC, Cheng CJ, Chi CW, Liu TY. Expression of cyclooxygenase-2 in prostate adenocarcinoma and benign prostatic hyperplasia. *Anticancer Res.* 2001; 21:1291–1294. [PubMed: 11396201]
5. Rouzer CA, Marnett LJ. Structural and functional differences between cyclooxygenases: fatty acid oxygenases with a critical role in cell signaling. *Biochem. Biophys. Res. Commun.* 2005; 338:34–44. [PubMed: 16126167]
6. Miller CC, McCreedy CA, Jones AD, Ziboh VA. Oxidative metabolism of dihomogammalinolenic acid by guinea pig epidermis: evidence of generation of anti-inflammatory products. *Prostaglandins.* 1988; 35:917–938. [PubMed: 3141974]
7. Das UN. Nutrients, essential fatty acids and prostaglandins interact to augment immune responses and prevent genetic damage and cancer. *Nutrition.* 1989; 5:106–110. [PubMed: 2520267]
8. Fan YY, Ramos KS, Chapkin RS. Cell cycle related inhibition of mouse vascular smooth muscle cell proliferation by prostaglandin E₁: relationship between prostaglandin E₁ and intracellular cAMP levels. *Prostaglandins Leukot Essent Fatty Acid.* 1996; 54:101–107.
9. Gianetti J, De Caterina M, de Cristofaro T, Ungaro B, Del Guercio R, De Caterina R. Intravenous prostaglandin E₁ reduces soluble vascular cell adhesion molecule-1 in peripheral arterial obstructive disease. *Am. Heart J.* 2001; 142:733–739. [PubMed: 11579367]
10. Takai S, Jin D, Kawashima H, Kimura M, Shiraishi-Tateishi A, Tanaka T, Kakutani S, Tanaka K, Kiso Y, Miyazaki M. Anti-atherosclerotic effects of dihomogamma-linolenic acid in ApoE-deficient mice. *J. Atheroscler. Thromb.* 2009; 16:480–489. [PubMed: 19713674]
11. Smith WL, DeWitt DL, Garavito RM. Cyclooxygenases: Structural, Cellular, and Molecular Biology. *Annu. Rev. Biochem.* 2000; 69:145–182. [PubMed: 10966456]
12. Masferrer JL, Zweifel BS, Manning PT, Hauser SD, Leahy KM, Smith WG, Isakson PC, Serbert K. Selective inhibition of inducible cyclooxygenase 2 in vivo is anti-inflammatory and nonulcerogenic. *Proc. Natl. Acad. Sci. USA.* 1994; 91:3228–3232. [PubMed: 8159730]
13. Hamberg M, Samuelsson B. On the mechanism of the biosynthesis of prostaglandins E₁ and F_{1 α} . *J. Biol. Chem.* 1967; 242:5336–5343. [PubMed: 6070851]
14. Hamberg M, Samuelsson B. Oxygenation of unsaturated fatty acids by the vesicular gland of sheep. *J. Biol. Chem.* 1967; 242:5344–5354. [PubMed: 6070852]
15. Miyamoto T, Yamamoto S, Hayaishi O. Prostaglandin synthetase system - resolution into oxygenase and isomerase components. *Proc. Nat. Acad. Sci. USA.* 1974; 71:3645–3648. [PubMed: 4215082]
16. Nugteren DH, Hazelhof E. Isolation and properties of intermediates in prostaglandin biosynthesis. *Biochim. Biophys. Acta.* 1973; 326:448–461. [PubMed: 4776443]
17. Yu Q, Purwaha P, Ni K, Sun C, Mallik S, Qian SY. Characterization of novel radicals from COX-catalyzed arachidonic acid peroxidation. *Free Radic. Biol. Med.* 2009; 47:568–576. [PubMed: 19482075]
18. Buettner GR. In the absence of catalytic metals ascorbate does not autoxidize at pH 7: ascorbate as a test for catalytic metals. *J. Biochem. Biophys. Methods.* 1988; 16:27–40. [PubMed: 3135299]
19. Yu Q, Shan Z, Ni K, Qian SY. LC/ESR/MS study of spin trapped carboncentered radicals formed from in vitro lipoxigenase-catalyzed peroxidation of γ -linolenic acid. *Free Radic. Res.* 2008; 42:442–455. [PubMed: 18484409]

20. Shan Z, Yu Q, Purwaha P, Guo B, Qian SY. A combination study of spintrapping, LC/ESR and LC/MS on carbon-centred radicals formed from lipoxygenase-catalysed peroxidation of eicosapentaenoic acid. *Free Radic. Res.* 2009; 43:1–15.
21. Yu Q, Xiao Y, Ni K, Qian SY. Identification and characterization of carbon-centered free radicals formed from lipoxygenase-catalyzed lipid peroxidation of DLA. *Chinese J. Analytical Chem.* 2009; 37:1815–1819.
22. Albro PW, Knecht KT, Schroeder JL, Corbett JT, Marbury D, Collins BJ, Charles J. Isolation and characterization of the initial radical adduct formed from linoleic acid and α -(4-pyridyl-1-oxide)-N-tert-butyl nitron in the presence of soybean lipoxygenase. *Chem. Biol. Interact.* 1992; 82:73–89. [PubMed: 1312396]
23. Ortiz de Montellano PR, Augusto O, Viola F, Kunze KL. Carbon radicals in the metabolism of alkyl hydrazines. *J. Biol. Chem.* 1983; 258:8623. [PubMed: 6305994]
24. Buettner GR. Spin Trapping: EPR parameters of spin adducts. *Free Radic. Biol. Med.* 1987; 3:259–303. [PubMed: 2826304]
25. Qian SY, Yue GH, Tomer KB, Mason RP. Identification of all class of spin-trapped carbon-centered radicals in soybean lipoxygenase-dependent lipid peroxidation of ω -6 polyunsaturated fatty acids via LC/ESR, LC/MS, and Tandem MS. *Free Radic. Biol. Med.* 2003; 34:1017–1028. [PubMed: 12684086]
26. Qian SY, Guo Q, Mason RP. Identification of spin trapped carbon-centered radicals in soybean lipoxygenase-dependent peroxidation of ω -3 polyunsaturated fatty acids by LC/ESR, LC/MS, and Tandem MS. *Free Radic. Biol. Med.* 2003; 35:33–44. [PubMed: 12826254]
27. Porter, Ned A.; Funk, MaxO. Peroxy radical cyclization as a model for prostaglandin biosynthesis. *J. Org. Chem.* 1975; 40:3614–3615. [PubMed: 1185331]
28. Laneuville O, Breuer DK, Xu N, Huang ZH, Gage DA, Watson JT, Lagarde M, DeWitt DL, Smith WL. Fatty acid substrate specificities of human prostaglandin-endoperoxide H synthase-1 and -2. *J. Biol. Chem.* 1995; 270:19330–19336. [PubMed: 7642610]
29. Malkowshi MG, Ginell SL, Smith WL, Garavito RM. The productive conformation of arachidonic acid bound to prostaglandin synthase. *Science.* 2000; 289:1933–1937. [PubMed: 10988074]
30. Thuresson ED, Malkowski MG, Lakkides KM, Rieke CJ, Mulichak AM, Ginell SL, Garavito RM, Smith WL. Mutational and X-ray crystallographic analysis of the interaction of dihomo- γ -linolenic acid with prostaglandin endoperoxide H synthases. *J Biol Chem.* 2001; 276:10358–10365. [PubMed: 11121413]

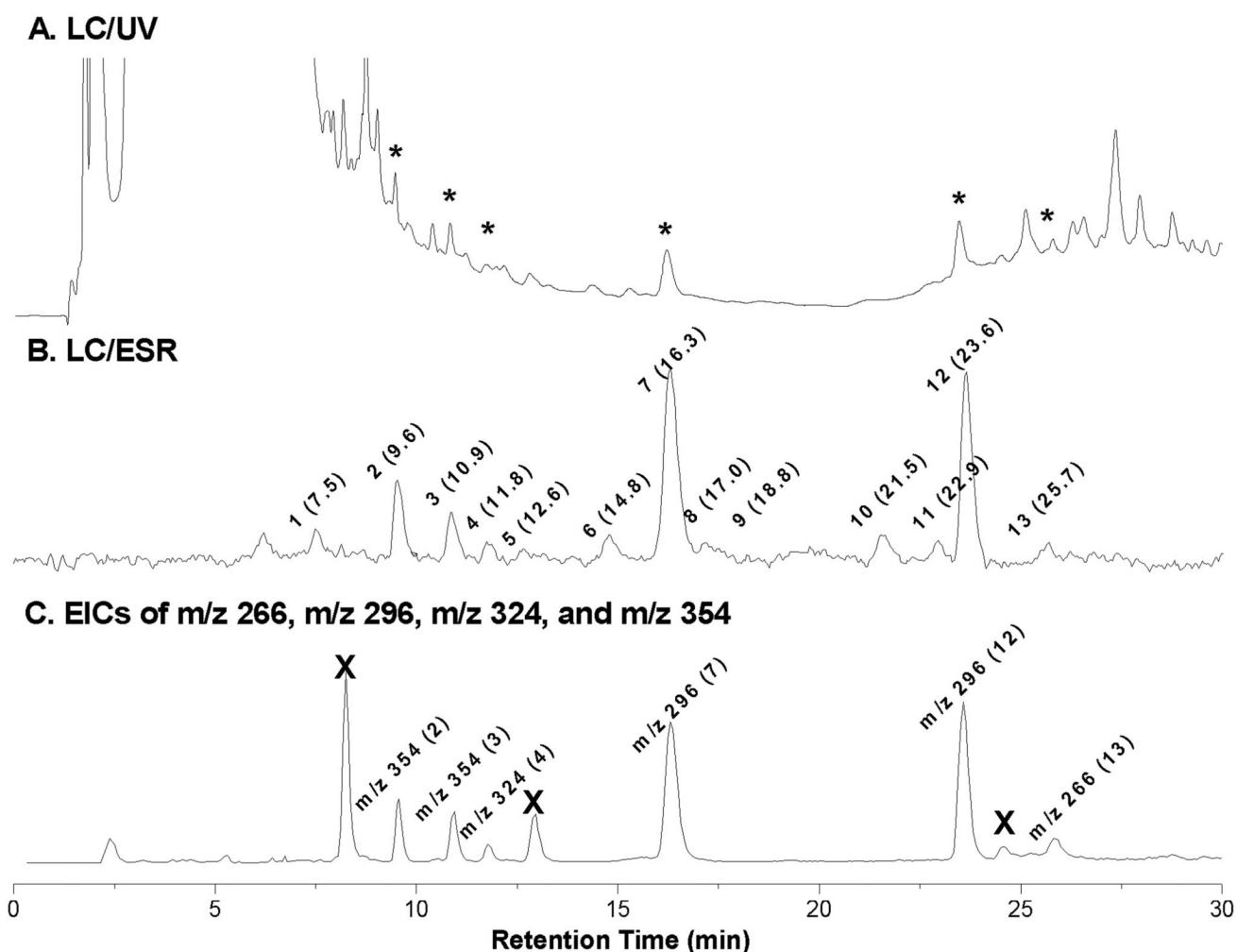


Figure 1. On-line LC/ESR and EIC of complete COX-DGLA reaction system. Reaction conditions (in Tris buffer, pH 8.0): 5 KUnit/mL COX (ovine), 2 mM DGLA, 5 μ M hydroquinone, 100 mM POBN, 50 μ M hematin at 37°C for 30 min. (A) UV chromatogram at 265 nm in HPLC with conditions of column and elution (gradient and isocratic) as described in detail under Materials and Methods; (B) ESR chromatogram with ESR magnetic field fixed on the maximum of the first line of the six-line signal. A total of thirteen ESR-active peaks are labeled with the corresponding retention time (min); and (C) Extracted ion current (EIC) chromatogram of m/z 266, m/z 296, m/z 324 and m/z 354 was projected from LC/MS of full scan (TIC of m/z 50 to m/z 600). EIC peaks are labeled with their MS as well as the corresponding LC/ESR-active peak numbers. Note that the peaks marked with 'x' were the radical-unrelated products sharing the same MS with some adducts since they are ESR-silent in B and the typical fragmentation pattern of POBN adduct could not be observed in their MS spectra (data not shown).

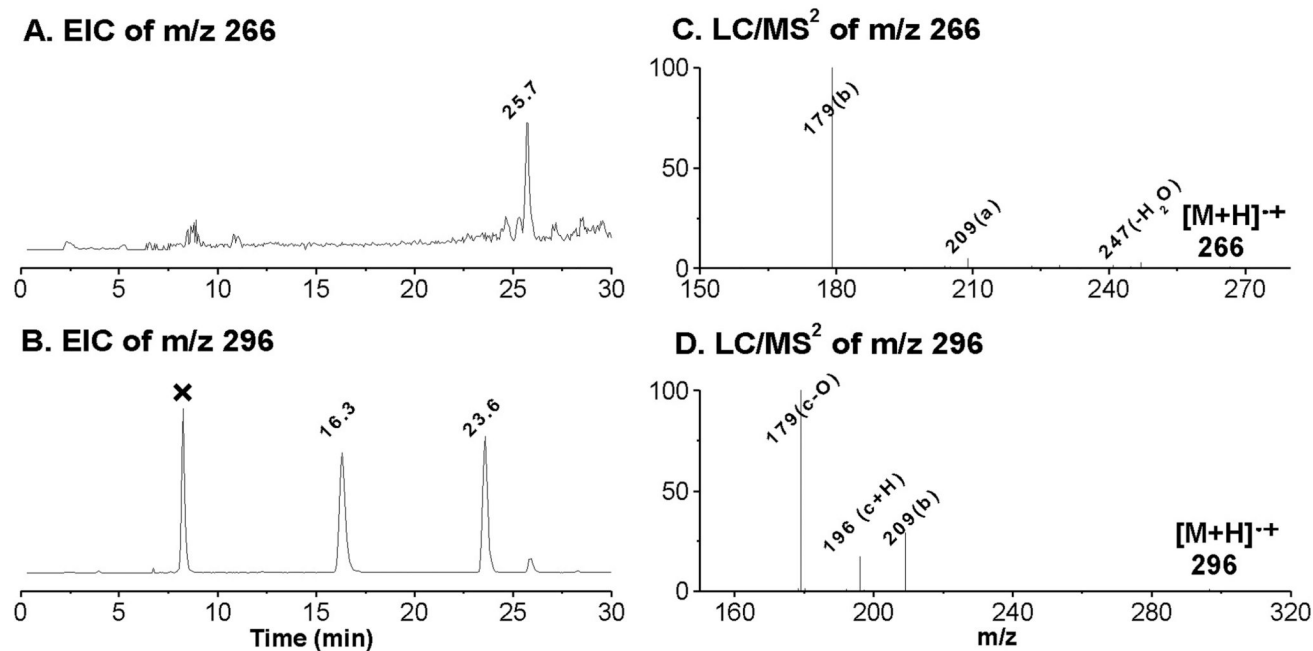


Figure 2. EICs and LC/MS² spectra of POBN adducts of m/z 266 and m/z 296 from the POBN spin-trapping experiment. (**A** and **B**) EIC of m/z 266 and m/z 296, respectively. Note that there are two isomers of m/z 296 as published previously [17], and that the peak marked with 'x' represents a radical-unrelated product since no such peaks could be obtained in the D₉-POBN spin-trapping experiment, nor could a typical fragmentation pattern of a POBN adduct be obtained in their MS spectra (data not shown); (**C** and **D**) LC/MS² of m/z 266 and m/z 296, respectively. The fragmentation pattern of each molecule is in agreement with patterns published previously [19,25].

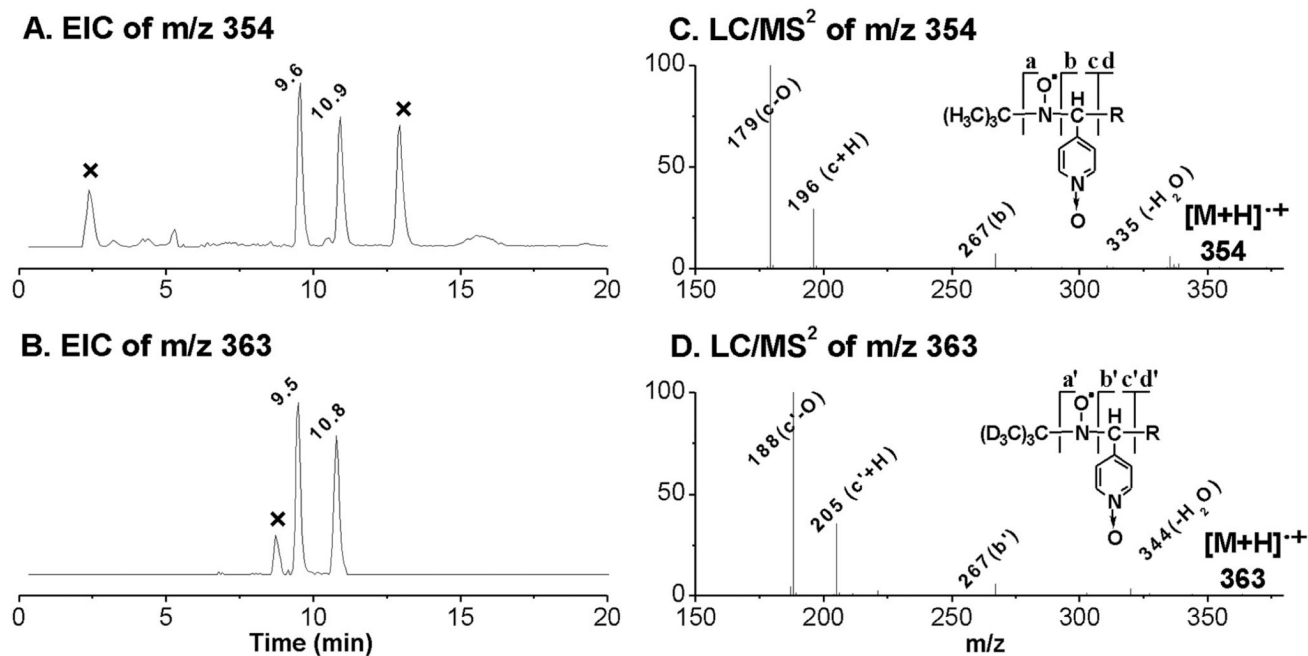


Figure 3. EICs and LC/MS² of D₀/D₉-POBN adducts of [•]C₈H₁₅O₃. (**A** and **B**) EIC of m/z 354 from the POBN spin-trapping experiment and EIC of m/z 363 from the D₉-POBN spin-trapping experiment, respectively. Note that two isomers of such a radical adduct were observed in both D₀/D₉-POBN trapping experiments with similar retention times, and that peaks marked with 'x' represent radical-unrelated products; (**C** and **D**) LC/MS² spectrum of m/z 354 from the POBN spin-trapping experiment and LC/MS² of m/z 363 from the D₉-POBN spin-trapping experiment, respectively. Note that *a* or *a'*, *b* or *b'*, *c* or *c'*, and *d* or *d'* ions represent typical fragmentation of POBN or D₉-POBN adducts in MS.

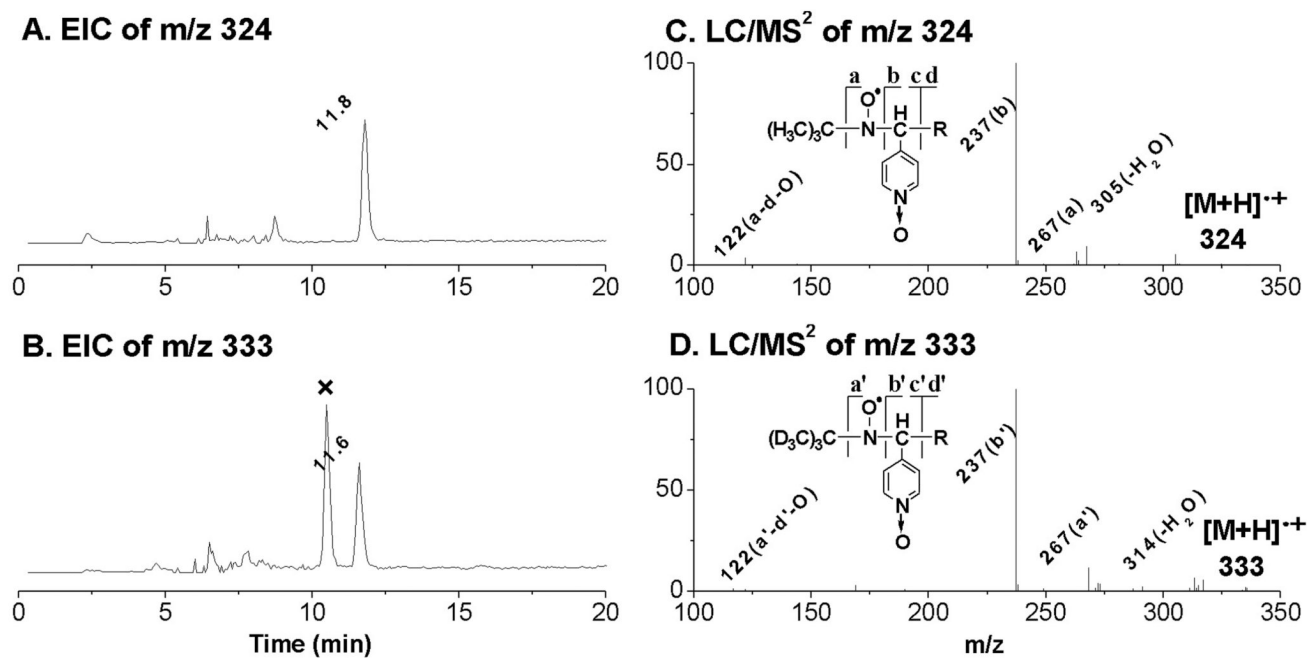
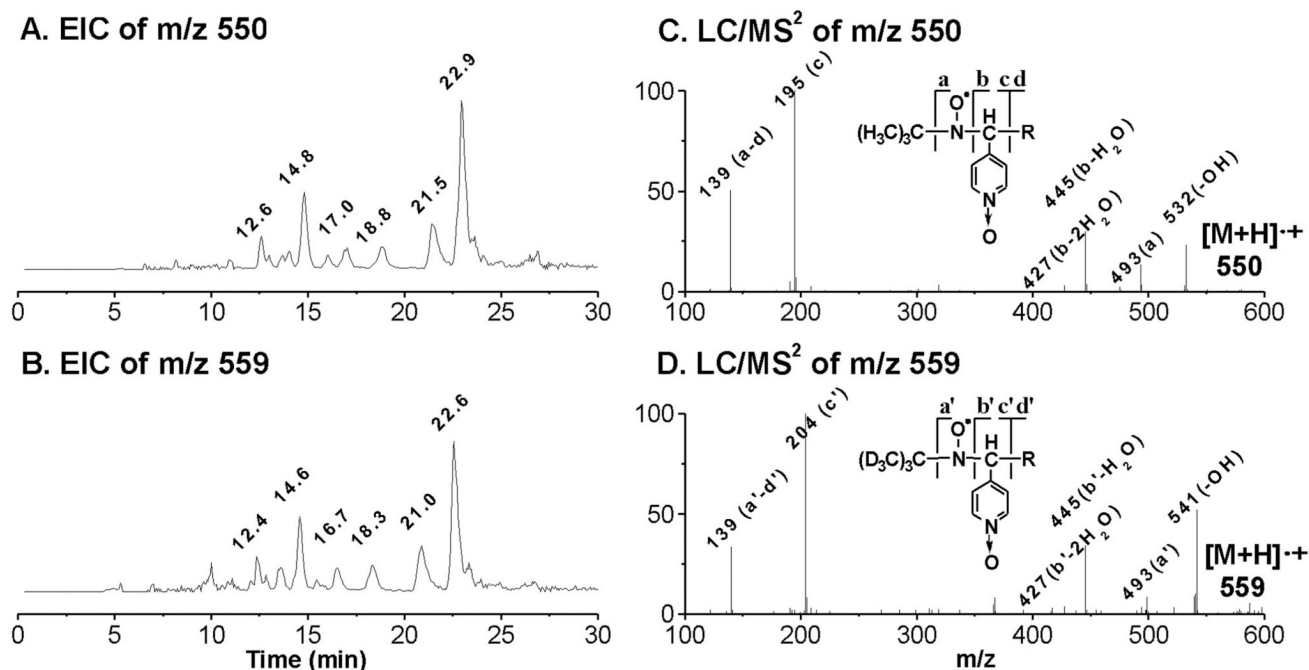


Figure 4. EICs and LC/MS² spectra of the D₀/D₉-POBN adducts of ¹³C₇H₁₃O₂. (**A** and **B**) EIC of m/z 324 from the POBN spin-trapping experiment and EIC of m/z 333 from the D₉-POBN spin-trapping experiment, respectively. Note that the peak marked with 'x' represents a radical-unrelated peak; (**C** and **D**) LC/MS² spectrum of m/z 324 from the POBN experiment and LC/MS² of m/z 333 from the D₉-POBN experiment, respectively. Note that *a* or *a'*, *b* or *b'*, *c* or *c'*, and *d* or *d'* ions are typical of fragmentation of POBN or D₉-POBN adducts in MS.

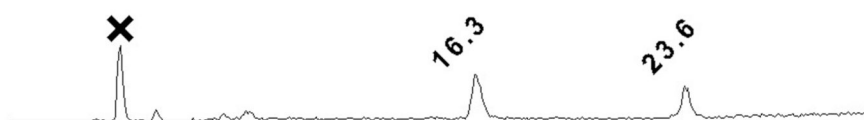
**Figure 5.**

EICs and LC/MS² of D₀/D₉-POBN adducts of •C₂₀H₃₅O₅. (**A** and **B**) EIC of m/z 550 from the POBN spin-trapping experiment and EIC of m/z 559 from the D₉-POBN spin-trapping experiment, respectively; (**C** and **D**) LC/MS² of m/z 550 from the POBN spin-trapping experiment and LC/MS² of m/z 559 from the D₉-POBN spin-trapping experiment, respectively. Note that *a* or *a'*, *b* or *b'*, *c* or *c'*, and *d* or *d'* ions are typical of fragmentation of POBN or D₉-POBN adducts in MS.

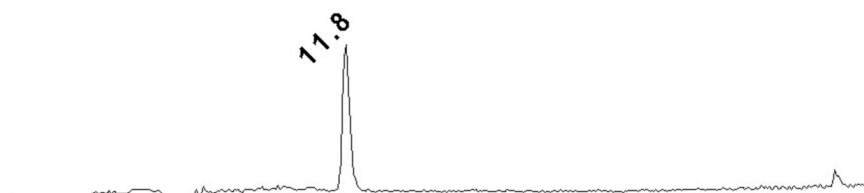
A. m/z 266 from HCA-7 Colony 29/DGLA



B. m/z 296 from HCA-7 Colony 29/DGLA



C. m/z 324 from HCA-7 Colony 29/DGLA



D. m/z 354 from HCA-7 Colony 29/DGLA

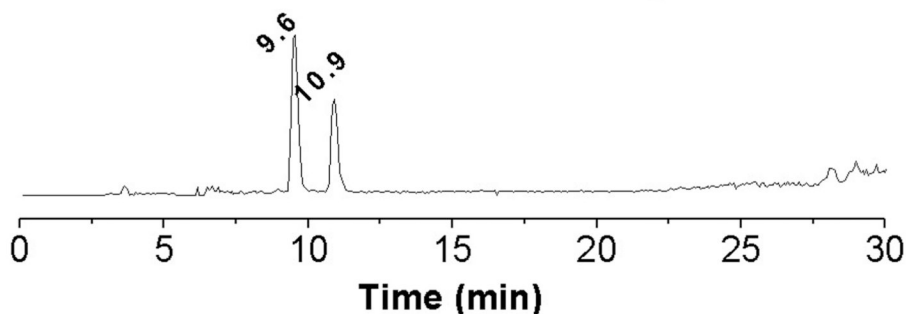
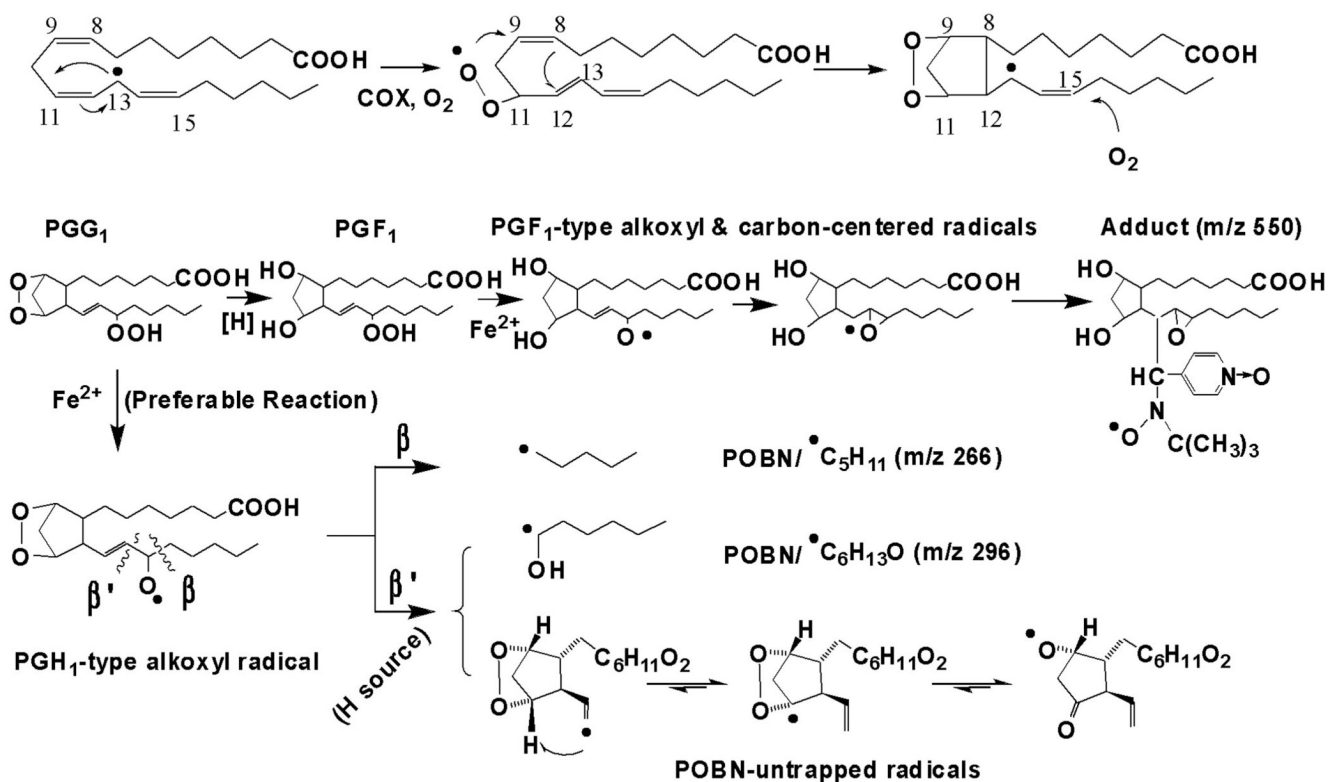


Figure 6.

EICs of m/z 266, m/z 296, m/z 324, and m/z 354 as POBN adducts of corresponding radicals detected in cellular peroxidation. Reaction conditions: radical adducts are generated from cells ($\sim 10^7$ cells/mL, HCT-7 colony 29)/PBS with addition of 50 mM POBN and 1.0 mM DGLA after an incubation of about 30 min. The reaction in the cells was stopped by adding ACN (1:1, v/v) and supernatant was then condensed for LC/MS analysis. (A) EIC of m/z 266; (B) EIC of m/z 296; (C) EIC of m/z 324; and (D) EIC of m/z 354. Note that retention as well as MS spectra from cell peroxidation all agreed with the LC/MS analysis of COX-DGLA in in vitro experiments in Figures 2–5, and that m/z 266, m/z 296, m/z 324, and m/z 354 could be detected at relatively low EIC intensities when 50 mM POBN as well

as 0.1, 0.25, and 0.5 mM DGLA were used in the cell-PBS incubation (cell viability of experiment of 1.0 mM to 0.1 mM DGLA was 90% to 10%, respectively).

COX-catalyzed C-9/C-11 endoperoxide formation, C-8/C-12 cyclization, and C-15 oxygenation to form PGG₁

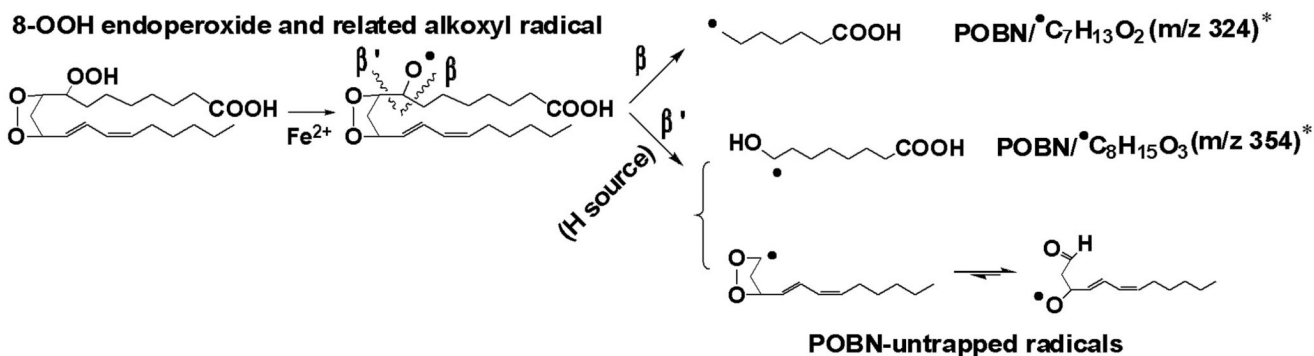
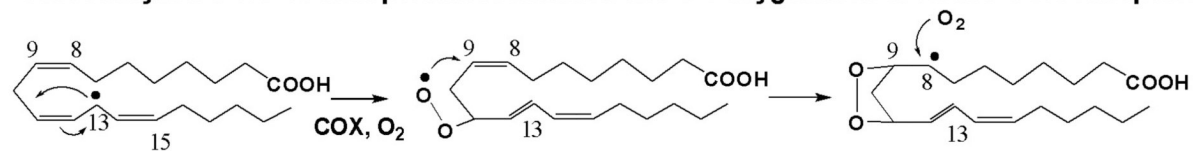


Scheme 1.

Proposed mechanism of COX-DGLA peroxidation to form DGLA-derived free radicals via C-15 oxygenation, a peroxidation pathway similar to COX-AA [17].

Note that in both COX-AA and DGLA peroxidation, free radical reactions including formation of C-13 radicals, C-9/C-11 endoperoxide bridge (addition of the first O₂), C-8 and C-12 cyclization, and C-15 oxygenation (via *peroxidase* activity of COX, addition of the second O₂). The source of H needed for the β'-scission in this pathway could be hydrophilic COX channel residues Tyr-385, Tyr-348, and Ser-530, as well as H₂O [29–30]. The proposed oxygen-centered radicals can be further decomposed to the other products, *e.g.* C-9 to C-11 elimination to form malonaldehyde.

COX-catalyzed C-9/C-11 endoperoxide formation and C-8 oxygenation to form 8-OOH endoperoxide



Scheme 2.

Proposed mechanism of COX-DGLA peroxidation to form DGLA-derived free radicals exclusively via C-8 oxygenation.

Note that in DGLA peroxidation, C-8 oxygenation (addition of the second O_2), after formation of the C-13 radical and C-9/C-11 endoperoxide bridge (addition of the first O_2), corresponds to the formation of carboxyl end carbon-centered radicals and oxygen-centered radicals. The H source needed for β' -scission in this pathway could be hydrophilic Ser-530 and Gly-526 of COX channel residues as well as H_2O [29–30]. The proposed oxygen-centered radicals can be further decomposed to the other products, *e.g.* C-9 to C-11 elimination to form malonaldehyde.

* In the case of peroxidation of DGLA-methyl ester, m/z 338 and m/z 368 of the POBN adduct of $^{\bullet}\text{C}_8\text{H}_{13}\text{O}_2$ ($^{\bullet}\text{CH}_2\text{OOCH}_3$) and $^{\bullet}\text{C}_9\text{H}_{17}\text{O}_3$ ($^{\text{HO}}\text{COOCH}_3$) are observed instead of m/z 324 and m/z 354.